Journal of Materials Chemistry C

Tailored Ligand Design Enabling Comprehensive Passivation of Perovskite Nanocrystals for Light-Emitting Diodes

Journal:	*Journal of Materials Chemistry C*
Manuscript ID	TC-ART-04-2025-001455.R1
Article Type:	Paper
Date Submitted by the Author:	05-Jun-2025
Complete List of Authors:	Kimura, Taisei; Yamagata University - Yonezawa Campus, Graduate school of science and engineering Yoshida, Kenshin; Yamagata University - Yonezawa Campus, Graduate School of Science and Engineering Narazaki, Kohei; Yamagata University - Yonezawa Campus, Graduate School of Organic Materials Science Yanagihashi, Kento; Yamagata University - Yonezawa Campus, Graduate School of Organic Materials Science Hirashima, Shun; Yamagata University - Yonezawa Campus, Graduate school of science and engineering Oyama, Yua; Yamagata University - Yonezawa Campus, Graduate school of science and engineering Thakuri, Khadga; University of Vermont, Department of Physics Ito, Yuta; Yamagata University - Yonezawa Campus, Graduate school of science and engineering Asakura, Satoshi; ISE Chemicals Corporation, Kashiwagi, Motofumi; ZEON Corporation White, Matthew; University of Vermont, Physical Chemistry Chiba, Takayuki; Yamagata University - Yonezawa Campus, Graduate School of Organic Materials Science Masuhara, Akito; Yamagata University - Yonezawa Campus, Graduate school of science and engineering

ARTICLE

Tailored Ligand Design Enabling Comprehensive Passivation of Perovskite Nanocrystals for Light-Emitting Diodes

Received 00th January 20xx,
Accepted 00th January 20xx

DOI: 10.1039/x0xx00000x

Taisei Kimura[a], Kenshin Yoshida[a], Kohei Narazaki[b], Kento Yanagihashi[b], Shun Hirashima[a], Yua Oyama[a], Khadga S Thakuri[c], Yuta Ito[a], Satoshi Asakura[d], Motofumi Kashiwagi[e], Matthew S White[c, f], Takayuki Chiba[b, g], and Akito Masuhara[a, g]*

Ever since the emergence of perovskite nanocrystals (PeNCs), their unique properties have attracted significant attention in both practical and academic fields, precisely because the ligands accentuate these characteristics. There are many examples of improving the optical properties, dispersibility, and durability of PeNCs by designing the ligands, and the usefulness of ligand engineering has been demonstrated. However, due to the emergence of highly complex issues stemming from the crystal and surface states of PeNCs, the harnessing of ligand design for LEDs—one of the major applications of PeNCs—remains limited. In this study, we focused on three aspects of the ligand's molecular structure: the head, tail, and counter anion, and by designing a structure that assigns distinct roles to each component, we comprehensively passivated the surface of PeNCs, thereby enabling their application in LEDs. The designed ligands relieved the crystal strain on the PeNCs, reduced the electrical insulation, and improved the optical properties by providing an ideal chemical surface. As a result of the synergistic effects, the EQE exhibits a 2.3-fold enhancement over the control devices, achieving a high value of 17.6%. This study not only proposes a ligand-engineering approach but also highlights this strategy as a new frontier in PeNCs research.

1. Introduction

Nanometer-sized semiconductor crystals are often called quantum dots, and they have unique optical properties that depend on their size. In addition, their surfaces are usually protected by organic molecules called ligands, which make it possible to stabilize and tune their properties.[1-3] They are referred to as perovskite nanocrystals (PeNCs) when the core consists of lead halide perovskite (composition formula: ABX_3, A = $CH(NH_2)_2^+$ (FA^+), $CH_3NH_3^+$ (MA^+), Cs^+; B = Pb^{2+}; X = Cl^-, Br^-, I^-). PeNCs demonstrate outstanding optical properties that distinguish them from conventional photoluminescent materials,[4] such as near-unity photoluminescence quantum yields (PLQY), ultra-narrow full width at half maximum (FWHM) of around 15–40 nm[5-7] in the emission spectrum, and their bandgap tunability across the entire visible range.[8, 9] These excellent optical properties are inherent to lead halide perovskite crystals and are enhanced by surface passivation by ligands. Ligands play a crucial role in determining the optical properties of the PeNCs. The role of the ligand is focused not only on the defect passivation and dispersibility of PeNCs,[10-13] but also the ligand greatly influences their morphology[14, 15] and electrical properties.[16-18] The importance is well known in the field of perovskite nanomaterials, and in recent years it has come to form a field of its own as ligand engineering.[19-24]

Despite the numerous studies that have focused on ligands as passivation strategies for the surface of PeNCs, the surface of PeNCs has always been a bottleneck in their performance and has hindered their application. These problems are particularly noticeable when PeNCs are applied in light-emitting diodes (LEDs). The causes of this restriction can be broadly classified into three categories: first, the formation of defects on the surface of the lead halide perovskite core; second, the crystal distortion caused by the strong surface tension inherent in nanomaterials; and finally, the insulating properties caused by the alkyl groups of the ligands. Lead halide perovskites are known as weak ionic crystals,[25] and the highly dynamic properties of their surfaces often have a negative impact on their nanomaterials.[26, 27] The elements of lead halide perovskite, especially halide ions, are easily desorbed from the surface, forming vacancy defects on it [28]. This creates deep trap levels within the band of PeNCs, inducing the non-radiative recombination of excitons. In addition, the surface of the PeNCs

[a] Graduate School of Science and Engineering, Yamagata University, 4-3-16, Jonan, Yonezawa, Yamagata 992-8510, Japan. E-mail: masuhara@yz.yamagata-u.ac.jp
[b] Graduate School of Organic Material Science, Yamagata University, 4-3-16, Jonan, Yonezawa, Yamagata 992-8510, Japan
[c] Department of Physics, The University of Vermont, Burlington, Vermont 05405, USA
[d] ISE CHEMICALS Corporation, 1-3-1 Kyobashi, Chuo-ku, Tokyo, 104-0031, Japan.
[e] ZEON Corporation, 1-6-2 Marunouchi, Chiyoda-ku, Tokyo, 100-8246, Japan.
[f] Material Science Program, The University of Vermont, Burlington, Vermont 05405, USA
[g] Research Center for Organic Electronics (ROEL), Yamagata University, 4-3-16 Jonan, Yonezawa, Yamagata, 992-8510, Japan.

Supplementary Information available: [Experimental methods, ^1H and ^{13}C NMR data of ligands, Details of evaluations of surface ligands, XRD profiles, optical properties of PeNCs, elemental analysis, and LED performance, Comparison of previous works]. See DOI: 10.1039/x0xx00000x

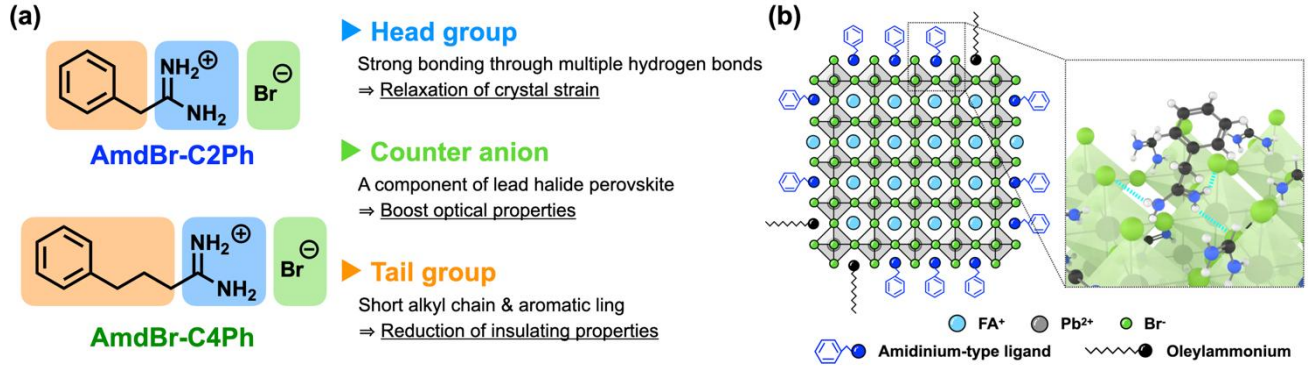

Fig. 1 (a) Schematic illustrations of the structures of AmdBr-C2Ph and AmdBr-C4Ph, and their design concepts. (b) Schematic illustrations of AmdBr-C2Ph adsorbed on the surface of $FAPbBr_3$ PeNCs.

is highly strained, which induces the formation of surface defects to relieve this strain. This is a common problem that arises because of the intrinsic flaw of nanomaterials.[29] Then, as is well-known, the major impact of the ligand is the insulating property of the alkyl group. The long alkyl groups contained in the ligands endow PeNCs with high dispersibility, but these long and continuous single carbon-to-carbon bonds exhibit strong insulating properties, which prevent the effective injection of carriers and become a barrier to their application in electroluminescent devices such as LEDs.[16, 18] As these previous studies illustrate, the surface of PeNCs is extremely complex, and utilizing the ligands—essential elements on the surface of PeNCs that enable comprehensive surface passivation—is a critical strategy to address these issues in a single decisive step.

Herein, we designed ligand molecules to overcome these issues from the three perspectives mentioned above and evaluated the effects of these molecules on PeNCs from multiple perspectives to clarify the effectiveness of the designed ligands. We assigned clear roles to the head, tail, and counter anion of the ligand, regarding it as a surfactant. These strategies led to an optimal surface of the PeNCs, and a significant improvement in performance was achieved by applying PeNCs to LEDs. There are three key factors in ligand design. First, we focused on the amidinium group as the adsorption head group for PeNCs, which enables strong passivation via multiple hydrogen bonds to halide ions on the surface of the PeNCs.[30-32] The bond between this head and the PeNCs can relax the crystal strain and suppress the formation of defects. Second, we synthesized the ligand as an amidinium salt with a bromide ion as the counter anion. This counter anion compensates for the halogen defects generated on the surface of PeNCs, eliminates the dangling bonds of lead, and thereby suppresses the formation of defect levels. As a result, it can effectively promote radiative recombination and improve the PLQY. Third, to reduce the insulating properties, a structure with a short alkyl chain length, *n* (*n* = 2 and 4), was selected as the framework. Additionally, an electron-delocalized aromatic ring was introduced to the end of the chain.[33, 34] These structures reduce the insulating properties and promote carrier injection into the nanocrystals, resulting in improved electrical properties. Following the aforementioned perspectives, the ligands were designed and synthesized, namely AmdBr-C2Ph (n = 2) and AmdBr-C4Ph (n = 4), as shown in Fig. 1(a). A combination of nuclear magnetic resonance (NMR), Fourier transform infrared spectroscopy (FT-IR), and X-ray diffraction (XRD) revealed that these molecules act as ligands for PeNCs. Furthermore, by consistently performing XRD analysis, elemental analysis, and optical property evaluation, as well as LED fabrication and evaluation, it was clarified that the head, tail, and counter anions of the ligand positively impact the characteristics of PeNCs. LEDs with these ligands successfully achieved a significant improvement in EQE, with a maximum of 17.6% for AmdBr-C2Ph, which was more than 10% higher than that of the control device. This research, which achieved these results ligand design and through a simple process of ligand exchange, demonstrates the further possibilities of ligand utilization.

2. Results and Discussion

2.1 General Evaluation of Perovskite Nanocrystals

In general, two types of ligands, carboxylic acid and amine, are used to prepare PeNCs,[8, 35, 36] and the charges are imparted by exchanging protons between them, and the ligands are adsorbed onto the PeNCs. However, when carboxylates and amines are exchanged by salt-type ligands, such as the designed ligands used in this study, they may act as a proton donor and remove the proton from the salt ligand (Fig. S3). Consequently, they lose their charge and are unable to form bonds with the PeNCs, inducing aggregation and a decrease in the optical properties of the PeNCs. To address this, we adopted oleylammonium bromide (OAmBr) as a single ligand (Fig. 2). This made it possible to introduce a designed ligand without damaging PeNCs. The AmdBr-C2Ph and AmdBr-C4Ph functionalized PeNCs are labelled AmdBr-C2Ph/PeNCs and AmdBr-C4Ph/PeNCs, respectively. For comparison, control PeNCs were prepared using only OAmBr and labelled as OAmBr/PeNCs.

The introduction of AmdBr-C2Ph and AmdBr-C4Ph to PeNCs was confirmed by ^{1}H NMR. ^{1}H NMR is one of the most useful methods for evaluating organic components such as surface

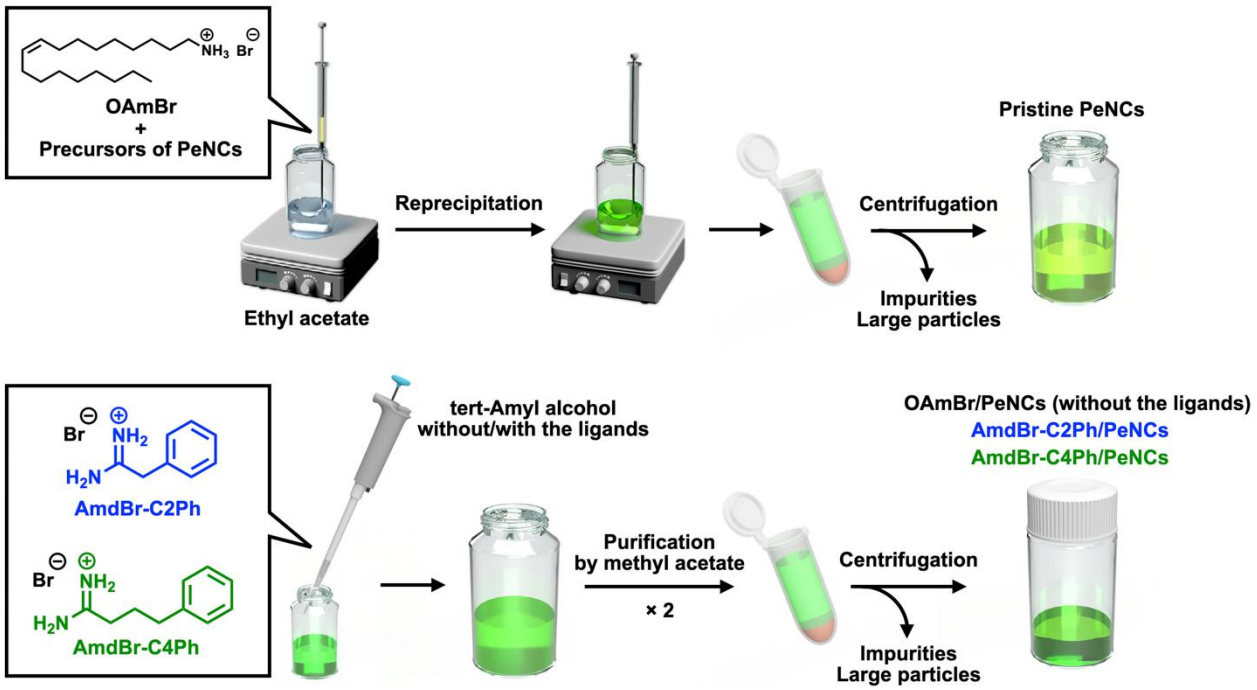

Fig. 2 Schematic illustration of the preparation, ligand exchange, and purification procedures of PeNCs in this work.

ligands. ^{1}H NMR spectra of the PeNCs, AmdBr-C2Ph, and AmdBr-C4Ph dissolved in DMSO-d_6 are shown in Fig. 3 (a) and (b). Three broad peaks observed at 9.01, 8.67, and 8.64 ppm in the spectra with PeNCs shown by the solid lines were attributed to protons on FA^+.[37] The peaks marked with † and ‡ in Fig. 3 (b) indicate protons on the nitrogen atoms of AmdBr-C2Ph and AmdBr-C4Ph, respectively, which were not observed in the OAmBr/PeNCs (The protons marked with † and ‡ are not equivalent. However, for this discussion, they are treated together. For detailed attribution, see Fig. S4 in Supporting Information.). However, these peaks were observed for AmdBr-C2Ph/PeNCs and AmdBr-C4Ph/PeNCs. These slight shifts in the peaks due to the presence or absence of PeNCs may have resulted from interactions between the metal residues and ligands in the solvent. Moreover, FT-IR also support the coordination of AmdBr-C2Ph and AmdBr-C4Ph to PeNCs (Fig. 3 (c)). In all samples, absorption peaks originating from FA^+ were observed at 3,405–3,171 cm^{-1} (N–H stretching), 1,711 cm^{-1} (C=N stretching), 1,570 cm^{-1} (N–H bending), and 1,352 cm^{-1} (C–N stretching).[38-40] In addition, peaks attributed to OAmBr appeared at 2,954 cm^{-1} (C–H stretching in methyl group), 2,920 and 2,850 cm^{-1} (C–H stretching in methylene group), and 1,464 cm^{-1} (the aliphatic stretching).[16, 41] Meanwhile, in the PeNCs with designed ligands, peaks were emphasized and observed at 1,680 cm^{-1} (C=N stretching), 839 cm^{-1} (C=N wagging), and 800 cm^{-1} (N–H bending), which are characteristic of these ligands.[42-44] Furthermore, peaks at 700 cm^{-1}, assigned to the C–H bending of the aromatic ring in the tail group, were also observed.[33] During the preparation of PeNCs, the PeNCs were thoroughly purified with methyl acetate to remove any free ligands that were not bound to the PeNCs. In other words, only ligands bound to the PeNCs could be observed in these spectra. These results revealed that AmdBr-C2Ph and AmdBr-C4Ph bind to the surface of PeNCs and act as ligands. In addition, the rates of OAmBr with AmdBr-C2Ph and AmdBr-C4Ph were estimated based on the quantifiability of the integral values of the ^{1}H NMR spectra. The rates of OAmBr with AmdBr-C2Ph and AmdBr-C4Ph were calculated to be 49% and 51%, respectively (Fig. S5).

The crystal structure was evaluated by XRD to clarify the effect of designed ligands on the structure. All the samples exhibited a typical cubic crystal of $FAPbBr_3$,[45, 46] independent of the ligand species, as shown in Fig. 3 (d). Designed ligands were introduced into the PeNCs by post-treatment, commonly referred to as ligand exchange (Fig. 2). The crystal structure was determined solely by the presence of OAmBr during nucleation. Thus, it is confirmed that they exist on the surface of the PeNCs without causing crystal structure distortion. Therefore, designed ligands were selectively present on the surface of the PeNCs and acted as ligands, as indicated by the NMR and XRD results. Furthermore, the morphology of the PeNCs, both as single particles and in ensembles, was evaluated by transmission electron microscopy (TEM) and dynamic light scattering (DLS). The TEM images and size distributions are shown in Fig. 3 (e)-(g). The particles exhibited a nearly uniform size and cubic shape, which was likely due to the independence of the crystal structure from the ligand. However, the size of the particles obtained from DLS was different from that measured directly from the TEM images. The size obtained from DLS refers to the hydrodynamic diameter of a particle, including its

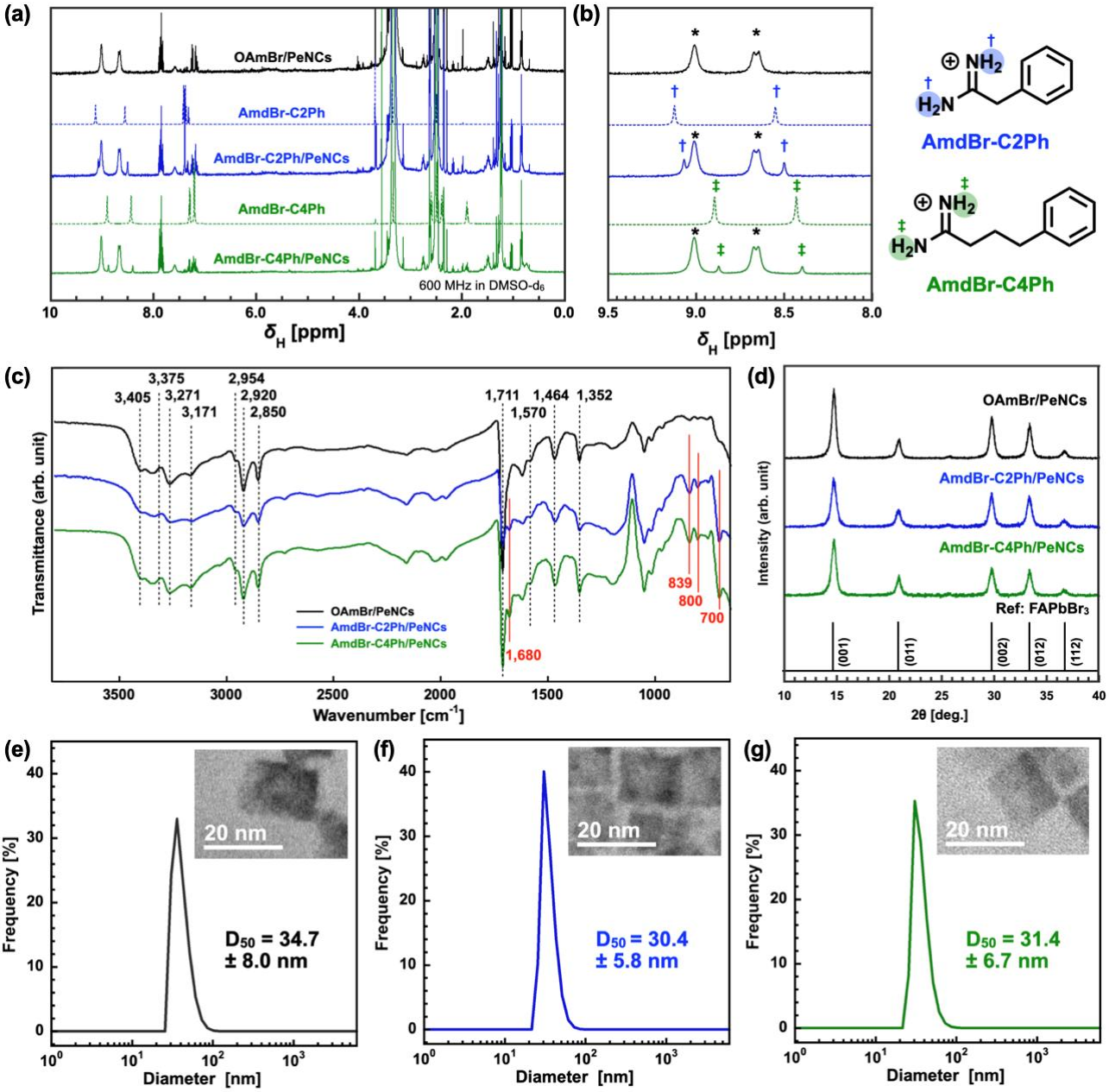

Fig. 3 (a) ^{1}H NMR spectra of the free ligand and system containing the ligand and PeNCs. The former is shown as a broken line and the latter as a solid line (600 MHz, DMSO-d6). (b) Expanded ^{1}H NMR spectra in the downfield region (9.5–8 ppm) and peak assignments for the ligand structure. (c) FT-IR spectra of each PeNCs sample. The peaks highlighted in red are attributed to designed ligands. (d) XRD patterns for each sample and the typical $FAPbBr_3$ diffraction pattern, indicated by the black vertical line. For (e) OAmBr/PeNCs, (f) AmdBr-C2Ph/PeNCs, and (g) AmdBr-C4Ph/PeNCs, the particle size distribution, and the inset are the TEM images of the representative

movement. Therefore, the diameter is influenced by factors such as ligands. It is reasonable to assume that the decrease in particle size in DLS in the order of OAmBr/PeNCs, AmdBr-C4Ph/PeNCs, and AmdBr-C2Ph/PeNCs is influenced by the length of the ligand chains. [47]

2.2 The Contribution to Surface Properties

First, the electrostatic potentials (ESP) of AmdBr-C2Ph and AmdBr-C4Ph were estimated based on density functional theory (DFT) calculations using the Gaussian 16 program at the B3LYP/6-31G** level,[48] as shown in Fig. 4. These maps show that regions close to blue are electron deficient, and regions close to red are electron rich. Electron-deficient regions passivate the anionic defects of PeNCs, and electron-rich regions passivate the cationic defects of PeNCs. Because the amidinium group is clearly electron-deficient, this functional group suggests that it can passivate A-site vacancies among the defect sites of PeNCs. Furthermore, the structure of the amidinium group, in which nitrogen is bonded to hydrogen, supports the formation of hydrogen bonds with halogens on the surface of the PeNCs.

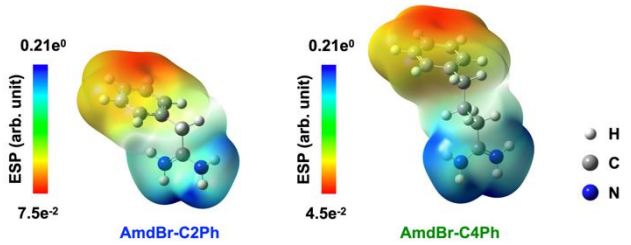

Fig. 4 Schematic illustration of the calculated ESP maps for AmdBr-C2Ph and AmdBr-C4Ph.

The effect of the amidinium group was evaluated by observing the crystal strain. Crystal strain exists in nanocrystals and quantum dots because of their extremely strong size confinement. The XRD has been established a firm position as a powerful tool in the structural analysis of crystals, and the broadening of the diffraction peaks in the spectrum can be attributed to the crystal strain and crystallite size. Therefore, by analysing these spectra, it is possible to estimate the crystal distortion.[49] In particular, this study quantified the strain in PeNCs using the Halder-Wagner method,[50] which estimates the strain and crystallite size. This is a method for approximating the integral breadth of an XRD profile, which is described by the convolution of the Gaussian and Lorentzian functions, and for estimating the broadening owing to crystal distortion and crystallite size. The shape of each peak in an XRD profile can be parametrized using the following equation (1):

$$\left(\frac{\beta}{\tan\theta}\right)^2 = \frac{K\lambda}{D}\cdot\frac{\beta}{\tan\theta\cdot\sin\theta} + 16\varepsilon^2 \qquad (1)$$

where β, ϑ, K, λ, D, and ε are the integral breadth of diffraction patterns, half of diffraction angle, Scherrer constant, X-ray wavelength, crystallite size, and strain, respectively. The graphs of $(\beta/\tan\theta)^2$ versus $\beta/\tan\theta\cdot\sin\theta$ were plotted, and the strains were obtained from the intercept (Fig. S6 and Table S1). The OAmBr/PeNCs possessed a strain value of 0.25%, which was the result of the influence of the particle size. The strain of $CsPbBr_3$ nanocubes shown in previous research was 0.2%[51] and the obtained result is reasonable considering the differences in the composition and particle size. However, surprisingly, in the case of the PeNCs whose surfaces were passivated by designed ligands, the strain was 0% in both cases. This result indicates that the amidinium group can effectively passivate the surface of nanocrystals and eliminate their distortion. Notably, this effect is not influenced by the structure of the alkyl group and is determined solely by the head amidinium.

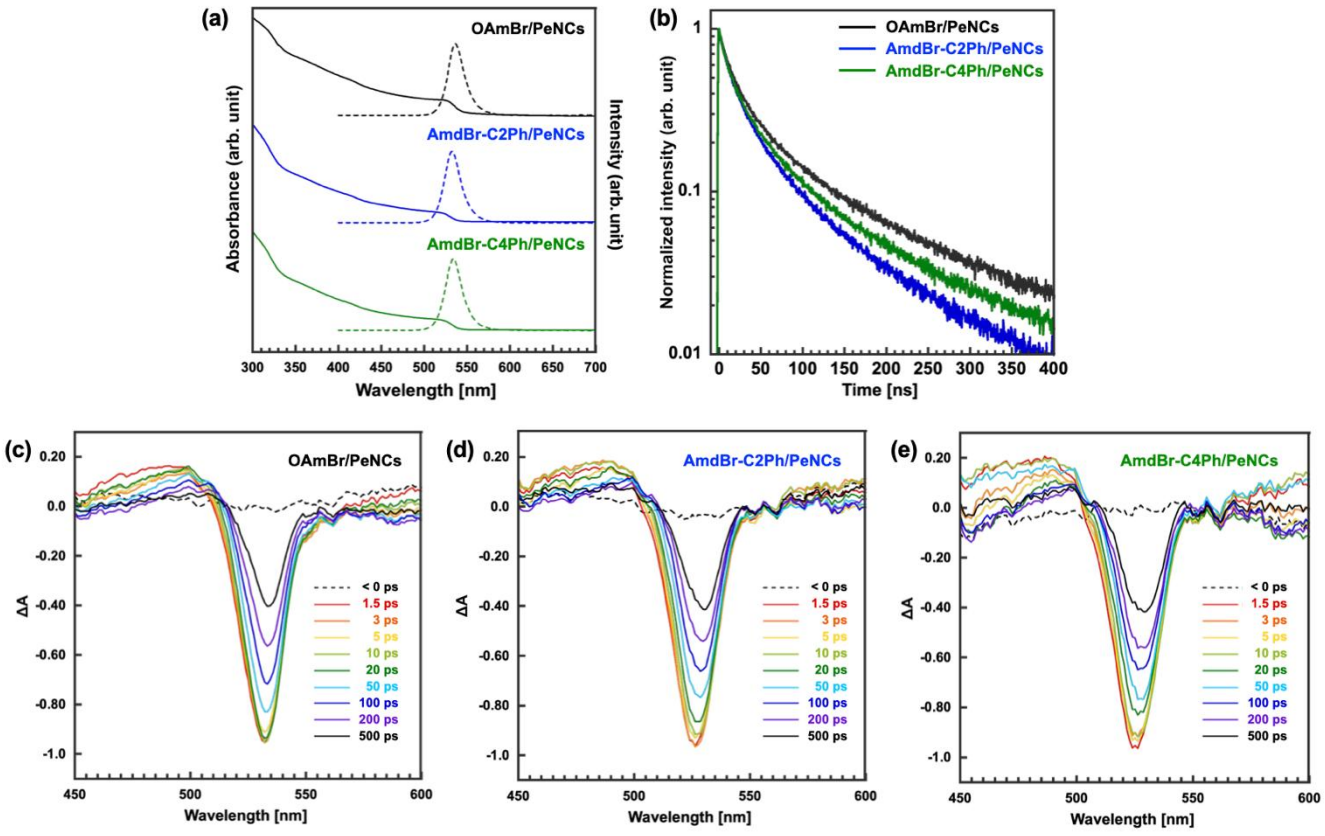

Fig. 5 (a) UV-vis absorption (solid line) and PL spectra (dashed line) and (b) TRPL decay curve of the obtained PeNCs. fs-TA profile of (c) OAmBr/PeNCs, (d) AmdBr-C2Ph/PeNCs, and (e) AmdBr-C2Ph/PeNCs at different probe delay times.

Table 1 The fitted constants (A_1 and A_2), average lifetimes (τ_{avg}), and faster (τ_1) and slower (τ_2) decay times of the PeNCs are shown in Fig. 5(b).

Sample	τ_{avg} [ns]	τ_1 [ns]	A_1	τ_2 [ns]	A_2	X^2
OAmBr/PeNCs	55.4	10.1	0.497	62.7	0.503	1.005
AmdBr-C2Ph/PeNCs	42.7	8.7	0.483	48.4	0.517	1.018
AmdBr-C4Ph/PeNCs	47.8	8.4	0.485	53.7	0.515	1.013

2.3 The Contribution to Optical Properties

The optical properties of the PeNCs are shown in Fig. 5 (a) and Table S2. OAmBr/PeNCs showed a relatively low 75% of PLQY, which is due to insufficient halogen defect passivation and excessive ligand removal by the washing solvent methyl acetate, leading to the formation of trap states in the band gap and inducing non-radiative recombination of excitons. On the other hand, AmdBr-C2Ph/PeNCs and AmdBr-C4Ph/PeNCs showed PLQYs of 88% and 91%, respectively, owing to the superior surface passivation of the PeNCs with designed ligands. These results were also supported by X-ray photoelectron spectroscopy (XPS), as shown in Fig. S7 and Table S3. Stoichiometrically, a ratio of Pb : halogen ions greater than 1:3 is preferable, as reported in previous studies on sufficiently defect-passivated PeNCs.[52-54] For OAmBr/PeNCs, AmdBr-C2Ph/PeNCs, and AmdBr-C4Ph/PeNCs, the ratios were 1:3.06, 1:3.43, and 1:3.30, respectively. Additionally, the Pb : N ratio from the added ligand increased. The bromide ions supplied to the system as counter anions for designed ligands can make the surface of PeNCs stoichiometrically ideal, eliminate trap levels, and improve their optical properties.

To obtain a deeper insight into the luminescence phenomenon, we measured time-resolved photoluminescence (TRPL). The TRPL decay curves obtained are shown in Fig. 5 (b) and were fitted with a biexponential function (Equation 2),

$$A(t) = A_1 \exp\left(-\frac{t}{\tau_1}\right) + A_2 \exp\left(-\frac{t}{\tau_2}\right) \quad (2)$$

where A_1 and A_2 are constant, t is time and τ_1 and τ_2 are the decay lifetimes, allowing for the determination of the faster recombination (τ_1) and slower recombination (τ_2) times. The average lifetime (τ_{avg}) was calculated using Equation (3).

$$\tau_{\text{avg}} = \frac{A_1\tau_1^2 + A_2\tau_2^2}{A_1\tau_1 + A_2\tau_2} \quad (3)$$

In general, it has been reported that the PL decay time tends to increase due to the passivation of the trap states.[30, 53, 55, 56] However, the increase in PLQY due to surface passivation by designed ligands did not correspond to an increase in the PL decay time (Fig. 5 (b) and Table 1). With respect to TRPL, the bleach recovery was slower in the femtosecond transient absorption (fs-TA) spectrum, contrary to the improvement in PLQY, and the behaviour was the same as that of the control sample (Fig. 5 (c)-(e)). These results suggest that the binding energy of the excitons increased owing to the dielectric confinement effect, [57, 58] which was caused by the formation of a dense ligand shell on the surface upon the addition of the designed ligand, leading to a decrease in the dielectric constant around the PeNCs. The amount of ligand was measured from ^{1}H NMR spectra, and it was found that the total amount of ligand in the system was 1.7 times higher for AmdBr-C2Ph/PeNCs and 1.9 times higher for AmdBr-C4Ph/PeNCs than for OAmBr/PeNCs (Fig. S5 and Table S4). This effect was consistent with the band-gap renormalization energy (ΔE_{rn}) calculated from the fs-TA spectra. AmdBr-C2Ph/PeNCs and AmdBr-C4Ph/PeNCs exhibited higher ΔE_{rn} values than OAmBr/PeNCs (Fig. S8 and Table S5). A larger ΔE_{rn} indicates a stronger Coulomb interaction, meaning that excitons possess a higher binding energy[59, 60]. Furthermore, by fitting the photobleaching peak with a biexponential model, it became clear that the recovery dynamics were accelerated as a result of surface modification of the PeNCs (Fig. S9 and Table S6).[61] These trends are consistent with the changes in the fluorescence properties.

These results show that counter anions contribute to improving optical properties and forming an ideal surface state. In addition, it was also found that the addition of a ligand during the post-treatment stage is strategically significant.

2.4 The Contribution to LED performance

Finally, to demonstrate the influence of the ligand on the electroluminescence properties of the PeNCs, LEDs were fabricated, and their performance was evaluated. To evaluate the effect of the ligand, we adopted a general device structure consisting of ITO/PEDOT:PSS with Nafion (40 nm)/PVK (20 nm)/PeNCs/TPBi (50 nm)/Liq (1 nm)/Al (100 nm). The electroluminescence (EL) spectra, current density–voltage, luminance–voltage, and EQE–current density characteristics are shown in Fig. 6, and the properties are summarized in Table S7. The EL spectra and FWHM were almost identical for all surface ligand conditions. The turn-on voltage decreased significantly as the alkyl chain length decreased, and it dropped to 3.1 V for AmdBr-C2Ph/PeNCs and 3.2 V for AmdBr-C4Ph/PeNCs from 3.7 V for OAmBr/PeNCs. As in previous studies,[16, 23, 62] this indicates that the short chain and aromatic ring of the ligand enable efficient charge injection. The short-tail and structural ingenuity resulted in a reduction in the turn-on voltage.

Eventually, the beneficial effects of ligand design are clearly evident in the EQE. The EQE for OAmBr/PeNCs was 7.6%, that for AmdBr-C4Ph/PeNCs was 11.6%, and that for AmdBr-C2Ph/PeNCs reached 17.6%, which is 2.3 times higher than that of the control sample. To support these remarkable improvements in the properties, we evaluated morphology of

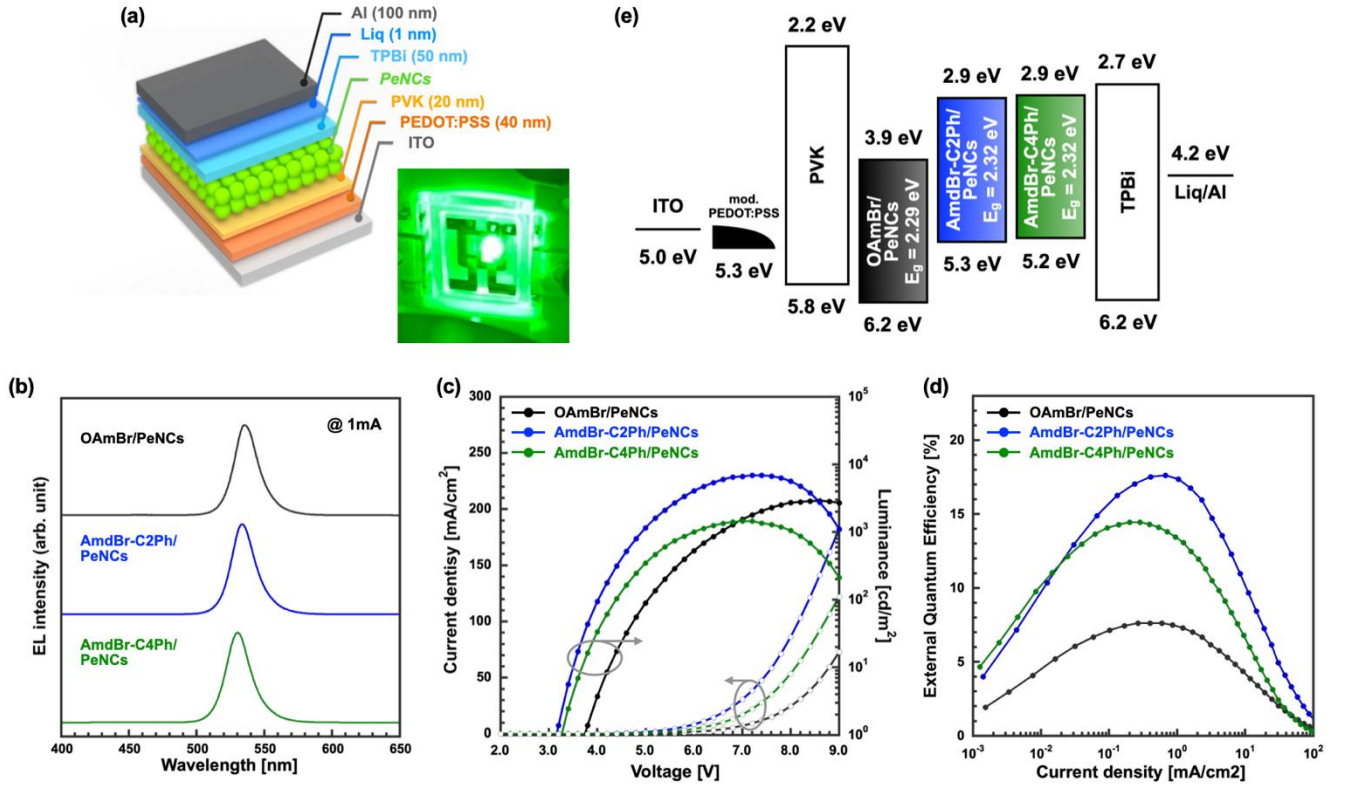

Fig. 6 (a) Schematic of the PeNCs LED structure (inset: fabricated PeNCs LED in operation). (b) EL spectra at 1 mA·cm^{-2}, (c) current density–voltage, (d) luminance–voltage, and (e) external quantum efficiency–current density characteristics.

the PeNCs thin films and energy levels of LEDs. Based on the morphological evaluation, no notable ligand-dependent changes were observed (Figure S10, Figure S11, Table S7, and Table S8), indicating that the improvement in LED performance was driven by the ligands. These findings are also supported by UPS measurements (Fig. 6(e)). In particular, for AmdBr-C2Ph/PeNCs and AmdBr-C4Ph/PeNCs, both the conduction and valence bands shifted by approximately 1 eV. As a result, the hole injection barrier was reduced, and the electron energy level was aligned with that of the electron-transport layer, leading to a drastic enhancement of LED performance. In previous research on PeNCs LEDs, a better EQE was achieved by modifying the device structure and/or doping with the lead halide perovskite crystal. In this study, the EQE was drastically improved by 10% compared with the same LED structure of the control PeNCs, simply by exchanging the ligands without modifying the device and core crystals. Since the properties of LEDs arise from the complex interplay of the entire material, this result was achieved due to the synergistic effects of not only the alkyl chain in the ligand's tail but also the optimal formation of the crystalline surface structures by the head group and the elimination of defects by the counter anion. Notably, to the best of our knowledge, the EQE achieved in this study is the highest reported for research involving ligand design although research on the design and synthesis of ligands is still limited, and examples of LED applications are also rare (Table S10 and S11). Even when compared to conventional PeNCs studies, the EQE improvement achieved through ligand exchange is relatively significant and noteworthy (Table S12). This result demonstrates the effectiveness of ligand design oriented toward comprehensive surface passivation.

3. Conclusions

In conclusion, we focused on the head, tail, and counter anions in the molecular structure of the ligand, and by designing that structure, we successfully achieved comprehensive passivation of the PeNCs surface. Based on three key considerations, we synthesized a designed ligand, demonstrated its function as a ligand, and clarified the beneficial effects it brings. Furthermore, we showed that by modifying an extremely small surface region of the nanocrystal, this ligand can simultaneously affect the crystal's structure, optical properties, and other characteristics. The amidinium groups in the head almost eliminated the distortion that occurs in the nanomaterials. In addition, the bromide ion, as a counter-anion, effectively passivated the dangling bonds of the lead ions on the surface, promoting the radiative decay of excitons. In addition, the short-chain alkyl group and the aromatic ring at the tail improved the electrical characteristics. In LEDs, the ligand exchanged PeNCs demonstrated a 16% reduction in turn-on voltage and a 2.3-fold higher EQE compared to PeNCs stabilized by the conventional ligand, oleylammonium bromide. The characteristics of PeNCs can be significantly enhanced not only through their inherent properties but also by optimizing the surface ligands and their structural design. This study provides

an example of such an approach and demonstrates its potential for advancing ligand engineering in the future.

Author contributions

Taisei Kimura – Conceptualization, Investigation, Methodology, Visualization, Writing – original draft; Kenshin Yoshida – Investigation, Methodology, Formal analysis, Visualization; Kohei Narazaki – Methodology, Formal analysis; Kento Yanagihashi – Methodology, Formal analysis; Shun Hirashima – Investigation, Data curation; Yua Oyama – Methodology, Data curation; Khadga S Thakuri – Formal analysis, Visualization; Yuta Ito – Software, Methodology; Satoshi Asakura – Funding acquisition, Resources; Motofumi Kashiwagi – Funding acquisition, Resources, Matthew S White – Funding acquisition, Supervision; Takayuki Chiba – Methodology, Formal analysis; Akito Masuhara – Project administration, Supervision, Writing – review & editing.

Conflicts of interest

There are no conflicts to declare.

Data availability

The data supporting this article have been included as part of the Supplementary Information.

Acknowledgements

The authors would like to thank “Grant-in-Aid for JSPS (Japan Society for the Promotion of Science) Fellows, JSPS KAKENHI Grant number 24KJ0450”, “JST (Japan Science and Technology Agency), the establishment of university fellowships towards the creation of science technology innovation, Grant Number JPMJFS2104”, “A-STEP (Adaptable and Seamless Technology transfer Program through Target-driven R&D) from JST, Grant Number JPMJTR223B”, and “Grant-in-Aid for Scientific Research(B), MEXT KAKENHI Grant number 22H01846”. This material is based upon work supported by the National Science Foundation under Grant No. OISE-2230706. Any opinions, findings, and conclusions or recommendations expressed are those of the authors and do not necessarily reflect the views of the National Science Foundation. This work was partially supported by JSPS Partnership for International research and Education (PIRE) Grant Number JPJSJRP20221201. The JSPS and NSF grants represent complementary funding in support of “US-Japan Partnership in Excitonic Soft Materials for Clean Energy”.

The JEOL JNM-EC500 and JEOL JSM-IT810 were introduced with the aid of a subsidy program for development of advanced research infrastructure.

References

1. F. P. Garcia de Arquer, D. V. Talapin, V. I. Klimov, Y. Arakawa, M. Bayer and E. H. Sargent, *Science*, 2021, **373**.
2. P. R. Brown, D. Kim, R. R. Lunt, N. Zhao, M. G. Bawendi, J. C. Grossman and V. Bulovic, *ACS nano*, 2014, **8**, 5863-5872.
3. D. M. Kroupa, M. Voros, N. P. Brawand, B. W. McNichols, E. M. Miller, J. Gu, A. J. Nozik, A. Sellinger, G. Galli and M. C. Beard, *Nat Commun*, 2017, **8**, 15257.
4. Y. Liu, Z. Ma, J. Zhang, Y. He, J. Dai, X. Li, Z. Shi and L. Manna, *Adv Mater*, 2025, DOI: 10.1002/adma.202415606, e2415606.
5. G. Raino, N. Yazdani, S. C. Boehme, M. Kober-Czerny, C. Zhu, F. Krieg, M. D. Rossell, R. Erni, V. Wood, I. Infante and M. V. Kovalenko, *Nat Commun*, 2022, **13**, 2587.
6. O. Chevalier, T. Nakamuro, W. Sato, S. Miyashita, T. Chiba, J. Kido, R. Shang and E. Nakamura, *J Am Chem Soc*, 2022, **144**, 21146-21156.
7. F. Liu, Y. Zhang, C. Ding, S. Kobayashi, T. Izuishi, N. Nakazawa, T. Toyoda, T. Ohta, S. Hayase, T. Minemoto, K. Yoshino, S. Dai and Q. Shen, *ACS Nano*, 2017, **11**, 10373-10383.
8. L. Protesescu, S. Yakunin, M. I. Bodnarchuk, F. Krieg, R. Caputo, C. H. Hendon, R. X. Yang, A. Walsh and M. V. Kovalenko, *Nano Lett*, 2015, **15**, 3692-3696.
9. R. Sato, Y. Morikawa, K. Yoshida, M. Goto, S. Asakura, M. Kashiwagi, T. Chiba and A. Masuhara, *ACS Applied Optical Materials*, 2024.
10. J. Pan, L. N. Quan, Y. Zhao, W. Peng, B. Murali, S. P. Sarmah, M. Yuan, L. Sinatra, N. M. Alyami, J. Liu, E. Yassitepe, Z. Yang, O. Voznyy, R. Comin, M. N. Hedhili, O. F. Mohammed, Z. H. Lu, D. H. Kim, E. H. Sargent and O. M. Bakr, *Adv Mater*, 2016, **28**, 8718-8725.
11. F. Krieg, S. T. Ochsenbein, S. Yakunin, S. Ten Brinck, P. Aellen, A. Suess, B. Clerc, D. Guggisberg, O. Nazarenko, Y. Shynkarenko, S. Kumar, C. J. Shih, I. Infante and M. V. Kovalenko, *ACS Energy Lett*, 2018, **3**, 641-646.
12. D. Yang, X. Li, W. Zhou, S. Zhang, C. Meng, Y. Wu, Y. Wang and H. Zeng, *Adv Mater*, 2019, **31**, e1900767.
13. V. Morad, A. Stelmakh, M. Svyrydenko, L. G. Feld, S. C. Boehme, M. Aebli, J. Affolter, C. J. Kaul, N. J. Schrenker, S. Bals, Y. Sahin, D. N. Dirin, I. Cherniukh, G. Raino, A. Baumketner and M. V. Kovalenko, *Nature*, 2024, **626**, 542-548.
14. T. Kimura, R. Yamakado, N. Oshita, S. Asakura and A. Masuhara, *Applied Physics Express*, 2022, **15**.
15. C. J. Dahlman, N. R. Venkatesan, P. T. Corona, R. M. Kennard, L. Mao, N. C. Smith, J. Zhang, R. Seshadri, M. E. Helgeson and M. L. Chabinyc, *ACS Nano*, 2020, **14**, 11294-11308.
16. T. Chiba, Y. Hayashi, H. Ebe, K. Hoshi, J. Sato, S. Sato, Y.-J. Pu, S. Ohisa and J. Kido, *Nature Photonics*, 2018, **12**, 681-687.
17. S. Mizoguchi, S. Sumikoshi, H. Abe, Y. Ito, R. Yamakado and T. Chiba, *ACS Omega*, 2024, **9**, 34692-34699.
18. Y. Tezuka, K. Umemoto, M. Takeda, Y. Takahashi, H. Ebe, J. Enomoto, S. Rodbuntum, T. Nohara, D. Fontecha, S. Asakura, T. Chiba, M. I. Furis, T. Yoshida, H. Uji-i and A. Masuhara, *Japanese Journal of Applied Physics*, 2020, **59**.
19. J. Park, H. M. Jang, S. Kim, S. H. Jo and T.-W. Lee, *Trends in Chemistry*, 2020, **2**, 837-849.
20. S. Ding, M. Hao, T. Lin, Y. Bai and L. Wang, *Journal of Energy Chemistry*, 2022, **69**, 626-648.
21. P. Li, X. Cao, J. Li, B. Jiao, X. Hou, F. Hao, Z. Ning, Z. Bian, J. Xi, L. Ding, Z. Wu and H. Dong, *Nanomicro Lett*, 2023, **15**, 167.

22. W. Sun, R. Yun, Y. Liu, X. Zhang, M. Yuan, L. Zhang and X. Li, *Small*, 2022, DOI: 10.1002/smll.202205950, e2205950.
23. J. H. Park, A. Y. Lee, J. C. Yu, Y. S. Nam, Y. Choi, J. Park and M. H. Song, *ACS Appl Mater Interfaces*, 2019, **11**, 8428-8435.
24. A. Islam, Z. Haider, M. Imran, M. D. Li and R. U. Hassan, *Advanced Optical Materials*, 2024, **13**.
25. A. K. Jena, A. Kulkarni and T. Miyasaka, *Chem Rev*, 2019, **119**, 3036-3103.
26. Y. Miao, Y. Chen, H. Chen, X. Wang and Y. Zhao, *Chem Sci*, 2021, **12**, 7231-7247.
27. J. De Roo, M. Ibanez, P. Geiregat, G. Nedelcu, W. Walravens, J. Maes, J. C. Martins, I. Van Driessche, M. V. Kovalenko and Z. Hens, *ACS Nano*, 2016, **10**, 2071-2081.
28. R. I. Biega and L. Leppert, *Journal of Physics: Energy*, 2021, **3**.
29. B. T. Sneed, A. P. Young and C.-K. Tsung, *Nanoscale*, 2015, **7**, 12248-12265.
30. Y.-H. Kim, S. Kim, A. Kakekhani, J. Park, J. Park, Y.-H. Lee, H. Xu, S. Nagane, R. B. Wexler, D.-H. Kim, S. H. Jo, L. Martínez-Sarti, P. Tan, A. Sadhanala, G.-S. Park, Y.-W. Kim, B. Hu, H. J. Bolink, S. Yoo, R. H. Friend, A. M. Rappe and T.-W. Lee, *Nature Photonics*, 2021, **15**, 148-155.
31. L. Lin, T. W. Jones, T. C.-J. Yang, X. Li, C. Wu, Z. Xiao, H. Li, J. Li, J. Qian, L. Lin, J. Q. Shi, S. D. Stranks, G. J. Wilson and X. Wang, *Matter*, 2024, **7**, 38-58.
32. H. Ebe, R. Suzuki, S. Sumikoshi, M. Uwano, R. Moriyama, D. Yokota, M. Otaki, K. Enomoto, T. Oto, T. Chiba and J. Kido, *Chemical Engineering Journal*, 2023, **471**.
33. E. T. Vickers, T. A. Graham, A. H. Chowdhury, B. Bahrami, B. W. Dreskin, S. Lindley, S. B. Naghadeh, Q. Qiao and J. Z. Zhang, *ACS Energy Letters*, 2018, **3**, 2931-2939.
34. J. Qiu, W. Xue, W. Wang and Y. Li, *Dyes and Pigments*, 2022, **198**.
35. F. Zhang, H. Zhong, C. Chen, X.-G. Wu, X. Hu, H. Huang, J. Han, B. Zou and Y. Dong, *ACS Nano*, 2015, **9**, 4533-4542.
36. K. Umemoto, H. Ebe, R. Sato, J. Enomoto, N. Oshita, T. Kimura, T. Inose, T. Nakamura, T. Chiba, S. Asakura, H. Uji-i and A. Masuhara, *ACS Sustainable Chemistry & Engineering*, 2020, **8**, 16469-16476.
37. W. T. M. Van Gompel, R. Herckens, G. Reekmans, B. Ruttens, J. D'Haen, P. Adriaensens, L. Lutsen and D. Vanderzande, *The Journal of Physical Chemistry C*, 2018, **122**, 4117-4124.
38. K. Hills-Kimball, Y. Nagaoka, C. Cao, E. Chaykovsky and O. Chen, *Journal of Materials Chemistry C*, 2017, **5**, 5680-5684.
39. A. Jana and K. S. Kim, *ACS Applied Energy Materials*, 2019, **2**, 4496-4503.
40. P. Wang, J. Guan, D. T. K. Galeschuk, Y. Yao, C. F. He, S. Jiang, S. Zhang, Y. Liu, M. Jin, C. Jin and Y. Song, *J Phys Chem Lett*, 2017, **8**, 2119-2125.
41. L. C. Cass, M. Malicki and E. A. Weiss, *Anal Chem*, 2013, **85**, 6974-6979.
42. S. Kumar, S. Raj, E. Kolanthai, A. K. Sood, S. Sampath and K. Chatterjee, *ACS Appl Mater Interfaces*, 2015, **7**, 3237-3252.
43. S.-N. Wang, F.-D. Zhang, A.-M. Huang and Q. Zhou, *Holzforschung*, 2016, **70**, 503-510.
44. T. Li, H. Zhang, C. Yu, P. Wang, H. Wang, X. Zhang, Y. Sun, D. Liu and T. Wang, *Journal of Materials Chemistry C*, 2021, **9**, 15488-15495.
45. A. Perumal, S. Shendre, M. Li, Y. K. E. Tay, V. K. Sharma, S. Chen, Z. Wei, Q. Liu, Y. Gao, P. J. S. Buenconsejo, S. T. Tan, C. L. Gan, Q. Xiong, T. C. Sum and H. V. Demir, *Scientific Reports*, 2016, **6**.
46. I. Levchuk, A. Osvet, X. Tang, M. Brandl, J. D. Perea, F. Hoegl, G. J. Matt, R. Hock, M. Batentschuk and C. J. Brabec, *Nano Lett*, 2017, **17**, 2765-2770.
47. B. J. Berne and R. Pecora, *Dynamic light scattering: with applications to chemistry, biology, and physics*, Courier Corporation, 2000.
48. M. J. Frisch, G. W. Trucks, H. B. Schlegel, G. E. Scuseria, M. A. Robb, J. R. Cheeseman, G. Scalmani, V. Barone, G. A. Petersson, H. Nakatsuji, X. Li, M. Caricato, A. V. Marenich, J. Bloino, B. G. Janesko, R. Gomperts, B. Mennucci, H. P. Hratchian, J. V. Ortiz, A. F. Izmaylov, J. L. Sonnenberg, Williams, F. Ding, F. Lipparini, F. Egidi, J. Goings, B. Peng, A. Petrone, T. Henderson, D. Ranasinghe, V. G. Zakrzewski, J. Gao, N. Rega, G. Zheng, W. Liang, M. Hada, M. Ehara, K. Toyota, R. Fukuda, J. Hasegawa, M. Ishida, T. Nakajima, Y. Honda, O. Kitao, H. Nakai, T. Vreven, K. Throssell, J. A. Montgomery Jr., J. E. Peralta, F. Ogliaro, M. J. Bearpark, J. J. Heyd, E. N. Brothers, K. N. Kudin, V. N. Staroverov, T. A. Keith, R. Kobayashi, J. Normand, K. Raghavachari, A. P. Rendell, J. C. Burant, S. S. Iyengar, J. Tomasi, M. Cossi, J. M. Millam, M. Klene, C. Adamo, R. Cammi, J. W. Ochterski, R. L. Martin, K. Morokuma, O. Farkas, J. B. Foresman and D. J. Fox, *Journal*, 2016.
49. D. Nath, F. Singh and R. Das, *Materials Chemistry and Physics*, 2020, **239**.
50. N. Halder and C. Wagner, *Acta Crystallographica*, 1966, **20**, 312-313.
51. T. Paul, B. K. Chatterjee, N. Besra, S. Thakur, S. Sarkar and K. K. Chattopadhyay, *Materials Today: Proceedings*, 2018, **5**, 2234-2240.
52. J. Song, T. Fang, J. Li, L. Xu, F. Zhang, B. Han, Q. Shan and H. Zeng, *Adv Mater*, 2018, **30**, e1805409.
53. T. Chiba, Y. Takahashi, J. Sato, S. Ishikawa, H. Ebe, K. Tamura, S. Ohisa and J. Kido, *ACS Appl Mater Interfaces*, 2020, **12**, 45574-45581.
54. K. Yoshida, N. Oshita, T. Kimura, M. Goto, R. Oikawa, M. Uwano, S. Asakura, T. Chiba and A. Masuhara, *Applied Physics Express*, 2024, **17**.
55. J. Chen, C. Zhang, X. Liu, L. Peng, J. Lin and X. Chen, *Photonics Research*, 2021, **9**.
56. Y. Zu, J. Xi, L. Li, J. Dai, S. Wang, F. Yun, B. Jiao, H. Dong, X. Hou and Z. Wu, *ACS Appl Mater Interfaces*, 2020, **12**, 2835-2841.
57. S. Kumar, J. Jagielski, N. Kallikounis, Y. H. Kim, C. Wolf, F. Jenny, T. Tian, C. J. Hofer, Y. C. Chiu, W. J. Stark, T. W. Lee and C. J. Shih, *Nano Lett*, 2017, **17**, 5277-5284.
58. O. Yaffe, A. Chernikov, Z. M. Norman, Y. Zhong, A. Velauthapillai, A. Van Der Zande, J. S. Owen and T. F. Heinz, *Physical Review B*, 2015, **92**, 045414.
59. C. Luo, C. Yan, W. Li, F. Chun, M. Xie, Z. Zhu, Y. Gao, B. Guo and W. Yang, *Advanced Functional Materials*, 2020, **30**.
60. N. Soetan, A. Puretzky, K. Reid, A. Boulesbaa, H. F. Zarick, A. Hunt, O. Rose, S. Rosenthal, D. B. Geohegan and R. Bardhan, *ACS Photonics*, 2018, **5**, 3575-3583.
61. K. Marjit, A. G. Francis, S. K. Pati and A. Patra, *J Phys Chem Lett*, 2023, **14**, 10900-10909.
62. S. Kumar, J. Jagielski, T. Marcato, S. F. Solari and C. J. Shih, *J Phys Chem Lett*, 2019, **10**, 7560-7567.

Tailored Ligand Design Enabling Comprehensive Passivation of Perovskite Nanocrystals for Light-Emitting Diodes

*Taisei Kimura, Kenshin Yoshida, Kohei Narazaki, Kento Yanagihashi, Shun Hirashima, Yua Oyama, Khadga S Thakuri, Yuta Ito, Satoshi Asakura, Motofumi Kashiwagi, Matthew S White, Takayuki Chiba, and Akito Masuhara**

Data availability statements

The data supporting this article have been included as part of the Supplementary Information.